micro

MDPI

Article

A Novel Approach of Polyethylene Glycol-4000 Hydrogels as Controlled Drug Carriers

Muhammad Suhail [1], I-Hui Chiu [1], I-Ling Lin [2,3], Ming-Jun Tsai [4,5,6,*] and Pao-Chu Wu [1,7,8,*]

1 School of Pharmacy, Kaohsiung Medical University, Kaohsiung 807, Taiwan; u108830004@kmu.edu.tw (M.S.); u110530002@kmu.edu.tw (I.-H.C.)
2 Department of Medicine Laboratory Science and Biotechnology, College of Health Science, Kaohsiung Medical University, Kaohsiung 807, Taiwan; linili@kmu.edu.tw
3 Department of Laboratory Medicine, Kaohsiung Medical University Hospital, Kaohsiung 807, Taiwan
4 School of Medicine, College of Medicine, China Medical University, Taichung 404, Taiwan
5 Department of Neurology, China Medical University Hospital, Taichung 404, Taiwan
6 Department of Neurology, An-Nan Hospital, China Medical University, Tainan 709, Taiwan
7 Department of Medical Research, Kaohsiung Medical University Hospital, Kaohsiung 807, Taiwan
8 Drug Development and Value Creation Research Center, Kaohsiung Medical University, Kaohsiung 807, Taiwan
* Correspondence: 22570@mtool.caaumed.org.tw or d22570@mail.cmuh.org.tw (M.-J.T.); pachwu@kmu.edu.tw (P.-C.W.); Tel.: +88-663-553-111 (ext. 1362) (M.-J.T.); +88-673-121-101 (P.-C.W.)

Abstract: In this study, we developed polyethylene glycol-4000-based hydrogels for ketorolac tromethamine-controlled delivery systems through a free radical polymerization method. The developed hydrogels were subjected to FTIR, TGA, DSC, XRD, SEM, porosity analysis, dynamic swelling analysis, release studies, etc. The successful crosslinking and stability of the prepared hydrogels were confirmed by FTIR, DSC, and TGA analysis. The surface morphology and the reduction in the crystallinity of the polymer after grafting were shown by SEM and XRD analysis. Similarly, the soluble part of the developed hydrogels was eliminated from their insoluble part by the Soxhlet extraction process. Higher dynamic swelling and drug release were observed at high pH values compared to low pH values. High porosity was perceived with high concentrations of the monomers and polymer and decreased with the high incorporation of a crosslinker. The release mechanism of all formulations followed non-Fickian diffusion. The results demonstrate that the developed polyethylene glycol-4000 hydrogels could serve as promising controlled drug delivery carriers.

Keywords: polyethylene glycol-4000 hydrogels; dynamic swelling analysis; porosity; in-vitro drug release

Citation: Suhail, M.; Chiu, I.-H.; Lin, I.-L.; Tsai, M.-J.; Wu, P.-C. A Novel Approach of Polyethylene Glycol-4000 Hydrogels as Controlled Drug Carriers. *Micro* **2023**, *3*, 578–590. https://doi.org/10.3390/micro3020039

Academic Editors: Laura Chronopoulou and Yujie Chen

Received: 13 April 2023
Revised: 19 May 2023
Accepted: 26 May 2023
Published: 1 June 2023

1. Introduction

Ketorolac tromethamine (KT) is a heteroaryl acetic acid derivative with analgesic and non-selective cyclooxygenase (COX) inhibitory effects, and is available on the market. The salt of ketorolac is tromethamine; thus, it is administered orally, intravenously, intramuscularly, and by topical ophthalmic application. The frequent complications of GI disturbances such as peptic ulceration, GI bleeding, and perforation, accompanied by a short half-life of about 5.5 h, have warranted the preparation of different formulation strategies to deliver KT in an appropriate way [1]. Therefore, various drug delivery systems have been developed for the sustained release of KT in a controlled fashion [1–3]. Wagh et al. (2019) synthesized ethyl cellulose-based micro/nanospheres for KT's controlled release [4]. Likewise, Patil and co-workers prepared chitosan nanoparticles for the sustained release of KT for up to 12 h [5]. However, challenges remain to be solved. Hydrogels are considered to be the most suitable carriers for the controlled release of active compounds due to their good biodegradability, biocompatibility, hydrophilicity, and non-toxicity [6].

Three-dimensional, hydrophilic, and polymeric networks called hydrogels have the capacity to absorb a lot of water or biological fluids [7,8]. Homopolymers or co-polymers

exist in these networks and are not soluble because of chemical or physical crosslinking [9]. Both physical integrity and network structure depend on chemical crosslinking. Thermodynamic compatibility with water is shown by these hydrogels, which enables them to swell in water [9,10]. The use of hydrogels is not only limited to clinical practice and experimental medicine; they are also used in regenerative medicine and tissue engineering [11], cellular immobilization, separation of cells or biomolecules, diagnostics, and in barrier materials to control biological adhesions. Currently, stimuli-sensitive hydrogels have attracted considerable attention in targeted drug delivery, as loaded molecules can be released by them at preferred positions in response to various minor environmental changes [12,13]. The pH of the human stomach is less than 3, whereas the pH of the intestine is greater than 6; this difference in pH is enough for hydrogels to behave in a pH-dependent manner [13–15].

Polyethylene glycol-4000 (PEG) is the most common polymer widely used to prepare targeted drug delivery systems. It is a synthetic polymer with no or very low toxicity and good biocompatibility. It is frequently combined with other polymers for the synthesis of controlled drug release systems [16]. Due to its rapid solidification rate, low melting point, high water solubility, low toxicity, availability in different molecular weights, and good physiological tolerance, it is generally employed as a vehicle. Hence, these features enable this polymer's use as a suitable agent to prepare drug delivery carriers [17]. Acrylic acid (AAc) is crucial for the synthesis of hydrogels. AAc-based hydrogels are commonly developed using the free radical polymerization method, because AAc reacts with the electrophilic agent and free radicals occur very easily. AAc is a synthetic monomer that prepares hydrogels by the crosslinking process with a greater quantity of water absorption as a single or multi-component system. Furthermore, AAc is used in combination with some other polymers to develop hydrogels of different types [18]. AMPS (2-acrylamido-2-methylpropanesulfonic acid) is a hydrophilic monomer existing in both non-ionic and ionic forms in nature. Its pKa value is almost 2. Due to its hydrophilic nature, the white crystalline powder AMPS dissolves very rapidly in water. Ionized sulfonate groups play a key role in the dynamic swelling ability of AMPS. The presence of sulfonic functional groups has enabled AMPS to show good resistance to hydrolysis and strong resistance to salt [19].

2. Materials and Methods

2.1. Materials

Ketorolac tromethamine was obtained from Jeedimetla, Hyderabad, Telangana, India. Ammonium persulfate (Aps) and acrylic acid were purchased from Showa (Tokyo, Japan) and Acros (Carlsbad, CA, USA), respectively. 2-acrylamido-2methylpropanesulfonic acid was acquired from Alfa Aesar (Lancashire, UK). Ethylene glycol dimethacrylate (EGDMA) was also procured from Alfa Aesar (Tewksbury, MA, USA).

2.2. Preparation of Hydrogels

Various combinations of PEG, AAc, AMPS, and EGDMA were crosslinked for the development of polyethylene glycol 4000-co-poly(acrylic acid/2-acrylamido-2-methylpropanesulfonic acid (PEG-co-p(AAc/AMPS)) hydrogels by the free radical polymerization technique, as shown in Table 1. Precise quantities of PEG and AMPS were dissolved in deionized distilled water. Ammonium persulfate (Aps) was dissolved in 1 mL of deionized distilled water. AAc and EGDMA were already available in liquid form. Aps solution was mixed with AMPS solution, which was poured into the polymer PEG solution. After proper mixing, AAc was added drop-wise to the aforementioned mixture, which further enhanced the polymerization reaction among the hydrogel contents. Finally, EGDMA was added to the mixture of polymer and monomers. The entire mixture was subjected to stirring for another 5 min. In order to remove the dissolved oxygen, nitrogen gas was used to purge the formed translucent solution. The solution was poured into glass molds, which were then submerged in a water bath at 55 °C for 2 h. The temperature was changed from 55 to 65 °C after the initial 2 h. The polymerization process was performed for 23 h. The

synthesized gel was cut into 8 mm discs, which were washed by a mixture of water and ethanol to remove any impurities attached to the surface of the prepared gel discs. The gel discs were exposed to atmospheric temperature for 24 h, and then placed in a vacuum oven at 40 °C for 7 days for complete dehydration. The dried hydrogel discs were assessed for further characterizations and studies. The proposed chemical structure of the developed hydrogel is given in Figure 1.

Table 1. Feed ratio scheme for formulations of PEG-co-p(AAc/AMPS) hydrogels.

F. Code	Polymer (PEG) g/100 g	Monomer (AAc) g/100 g	Monomer (AMPS) g/100 g	Initiator (Aps) g/100 g	Crosslinker (EGDMA) g/100 g
F-1	0.50	20	10	0.5	1.0
F-2	0.75	20	10	0.5	1.0
F-3	1.00	20	10	0.5	1.0
F-4	0.50	20	10	0.5	1.0
F-5	0.50	25	10	0.5	1.0
F-6	0.50	30	10	0.5	1.0
F-7	0.50	20	10	0.5	1.0
F-8	0.50	20	15	0.5	1.0
F-9	0.50	20	20	0.5	1.0
F-10	0.50	20	10	0.5	0.5
F-11	0.50	20	10	0.5	1.0
F-12	0.50	20	10	0.5	1.5

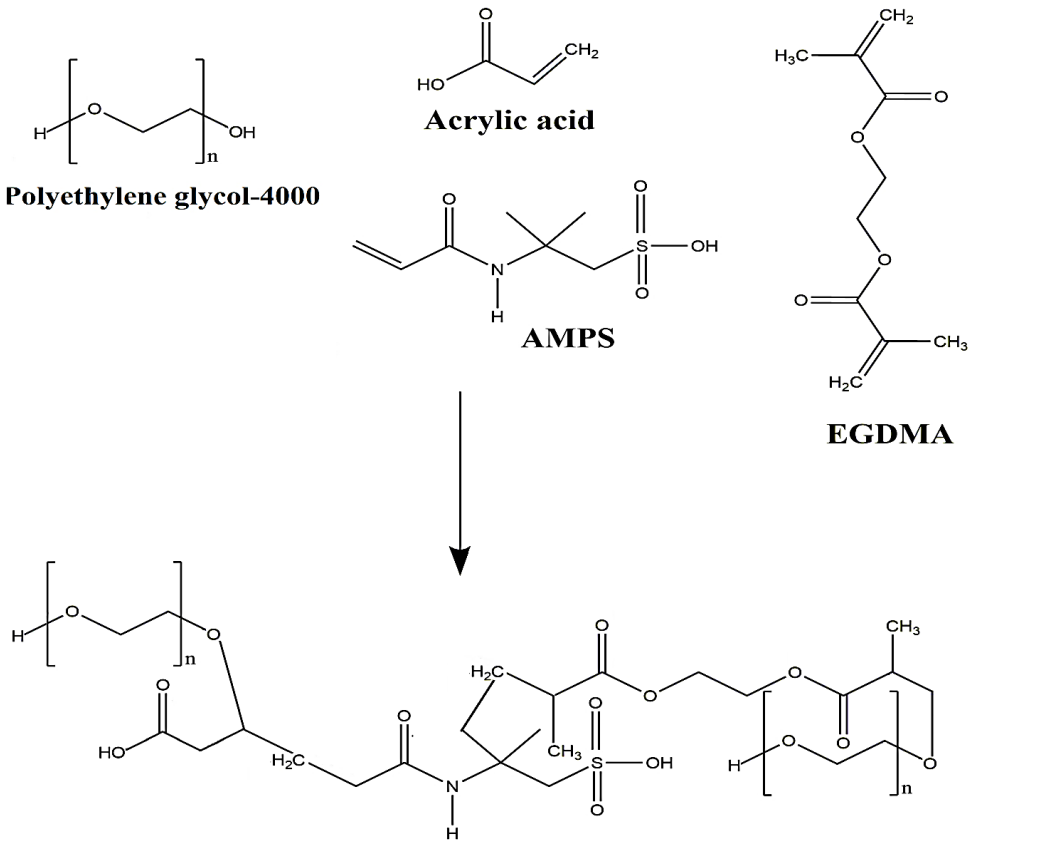

Figure 1. Proposed chemical structure of PEG-co-p(AAc/AMPS) hydrogel.

2.3. FTIR/TGA/DSC/XRD and SEM

The spectral analysis of PEG, AAc, AMPS, the unloaded hydrogel, Kt, and the drug-loaded hydrogel was performed by attenuated total reflectance (ATR) NICOLET 380 FTIR (Thermo Fisher Scientific, Ishioka, Japan) in the range of 4500–500 cm^{-1}. TGA (PerkinElmer

Simultaneous Thermal Analyzer STA 8000) was carried out at temperatures from 40 to 600 °C with a heating rate of 20 °C/min. Nitrogen flow was kept constant throughout the analysis [20]. Similarly, for DSC (PerkinElmer DSC 4000) analysis, the samples were scanned at temperatures from 50 to 400 °C at a heating rate of 20 °C/min with a constant nitrogen flow rate of 20 °C/min [21]. XRD (XRD-6000 Shimadzu, Tokyo, Japan) examination was performed with a heating rate of 2°/min and an angle range of 10 to 60° [22]. Likewise, the surface morphology of the prepared hydrogels was assessed at different magnifications through SEM (JSM-5300 model, JEOL, Tokyo, Japan) [23].

2.4. Sol–Gel Analysis

The Soxhlet extraction process was applied for the determination of uncrosslinked and crosslinked fractions of the prepared hydrogel. Thus, hydrogel discs of specified weights were taken and placed in the Soxhlet apparatus containing boiling water for 12 h. The extracted discs were taken out after the extraction procedure and kept in a vacuum oven at 40 °C to dry [24]. The following equations were employed for the determination of sol–gel fractions:

$$\text{Sol fraction\%} = \frac{F_1 - F_2}{F_1} \times 100 \quad (1)$$

$$\text{Gel fraction} = 100 - \text{Sol fraction} \quad (2)$$

F_1 represents the initial weight of the dried hydrogel disc, while F_2 is the final weight after the extraction process.

2.5. Porosity Study

The solvent displacement method was employed for the estimation of porosity of the PEG-co-p(AAc/AMPS) hydrogel, using absolute ethanol as a displacement solvent. Weighed dried discs of hydrogel (Z_1) of all formulations were placed in absolute ethanol for maximum penetration of ethanol into the hydrogel network for 72 h. Later, the hydrogel discs were taken out, the extra ethanol attached to the surface of the hydrogel discs was removed, and they were weighed again (Z_2) [25]. The (%) porosity was estimated by the following equation:

$$(\%)\ \text{Porosity} = \frac{Z_2 - Z_1}{\rho V} \times 100 \quad (3)$$

ρ is the density of absolute ethanol, while V represents the swelling volume of hydrogel discs.

2.6. Dynamic Swelling

Dynamic swelling of PEG-co-p(AAc/AMPS) hydrogels was investigated at three pH values of 1.2, 4.6, and 7.4, at 37 °C. A weighed dried hydrogel disc was immersed in a 100 mL buffer solution with pH values of 1.2, 4.6, and 7.4. After a predetermined amount of time, the disc was removed, blotted with filter paper, and weighed again. Swelling persisted until equilibrium swelling was attained [26]. This experiment was carried out in triplicate. The swelling index was estimated by the following equation:

$$(q) = \frac{L_2}{L_1} \quad (4)$$

q is the dynamic swelling, L_1 is the initial weight of the dried hydrogel discs before swelling, and L_2 is the final weight after swelling at time t.

2.7. In Vitro Drug Release Studies

In vitro drug release studies were performed for the commercially available product Keten and the developed hydrogels at three pH levels (1.2, 4.6, and 7.4) in a dissolution apparatus II (USP dissolution (Sr8plus Dissolution Test Station, Hanson Research, Chatsworth, CA, USA)). Loaded hydrogel discs and Keten were placed separately in 900 mL of dis-

solution medium with pH 1.2, 4.6, and 7.4 at 37 ± 0.5 °C and 50 rpm. Samples of 5 mL were collected at regular time intervals, and fresh medium of the same concentration was added back in to keep the sink conditions constant. The absorbance analysis of all collected samples was carried out using a UV–Vis spectrophotometer (U-5100, 3J2-0014, Tokyo, Japan) at ʎmax 280 nm in triplicate [27]. Similarly, kinetic models such as zero-order, first-order, Higuchi, and Korsmeyer–Peppas were computed to know the order and release mechanism of the drug from the PEG-co-p(AAc/AMPS) hydrogel. Release data were fixed to the respective kinetic models [28].

2.8. Statistical Analysis

ANOVA-test was used for the statistical analysis of the differences between the tests. Differences were statistically significant when the *p*-value was less than 0.05.

3. Results and Discussion

3.1. Preparation of PEG-Based Hydrogels

Polyethylene glycol 4000-co-poly(acrylic acid/2-acrylamido-2-methylpropanesulfonic acid (PEG-co-p(AAc/AMPS)) hydrogels were prepared. Various combinations of PEG, AAc, EGDMA, and AMPS were crosslinked in the presence of Aps. Figure 2 shows the physical appearance of the dried hydrogel discs.

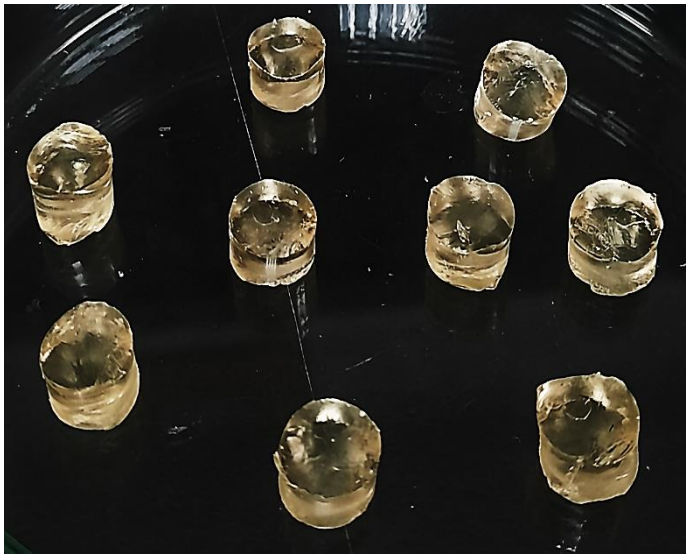

Figure 2. The physical appearance of PEG-co-p(AAc/AMPS) hydrogel discs.

3.2. FTIR Analysis

FTIR spectrum analysis was implemented to investigate the structural arrangement of PEG, AAc, AMPS, unloaded PEG-co-p(AAc/AMPS) hydrogels, KT, and loaded PEG-co-p(AAc/AMPS) hydrogels. FTIR spectra of PEG (Figure 3A) indicated the stretching vibration of –OH at 3268 cm^{-1}. A sharp peak at 2910 cm^{-1} indicated the stretching vibration of alkyl (–CH_2), while a peak at 1088 cm^{-1} indicated the stretching of the ether (C–O–C) group. The same peaks of PEG were shown by Patil and coworkers, which supports our results [29]. As shown in Figure 3B, the FTIR spectra of AAc showed bands at 1322, 1648, and 3007 cm^{-1}, indicating –C=O, –C–C, and –CH_2 stretching vibrations, respectively [30]. The FTIR spectra of AMPS (Figure 3C) revealed a sharp band at 3008 cm^{-1}, indicating C–H stretching of the methyl group, whereas absorption peaks at 1627 and 1678 depicted stretching and bending of N–H and C=O groups. Likewise, absorption bands of the S=O group were observed at 1152 and 1404 cm^{-1} [31]. Due to polymerization among hydrogel contents, a fluctuation was seen in the distinct bands of PEG, AAc, and AMPS, as demonstrated by FTIR spectra of the PEG-co-p(AAc/AMPS) hydrogel (Figure 3D). The

peaks of PEG and AAc at 2910, 1088 cm^{-1} and 1322, 1648 cm^{-1} were improved to 2970, 1140 cm^{-1} and 1350, 1675 cm^{-1} peaks of the unloaded PEG-co-p(AAc/AMPS) hydrogel. Likewise, a few peaks of AMPS at 1404, 1627 cm^{-1} were shifted to 1445, 1680 cm^{-1}. It was evident that AAc and AMPS had been grafted onto the backbone of PEG by the shifting, disappearance, and creation of some peaks, which depicted the synthesis of the PEG-co-p(AAc/AMPS) hydrogel. Characteristic peaks of KT (Figure 3E) were seen by its FTIR spectra at 1160, 1202, 1382, and 3372 cm^{-1}, demonstrating the stretching vibration of –C=O, OH, –C–N, NH_2, and N-H. C–H bending was observed with peaks at 2148 and 798 cm^{-1} [32–35]. Certain peaks of KT showed a minor change after being encapsulated in the prepared hydrogels. The distinct bands of KT at 1382 and 3372 cm^{-1} changed to 1406 and 3381 cm^{-1} for the KT-loaded PEG-co-p(AAc/AMPS) hydrogel (Figure 3F); thus, no interaction was observed between the KT and PEG-based hydrogel ingredients [36].

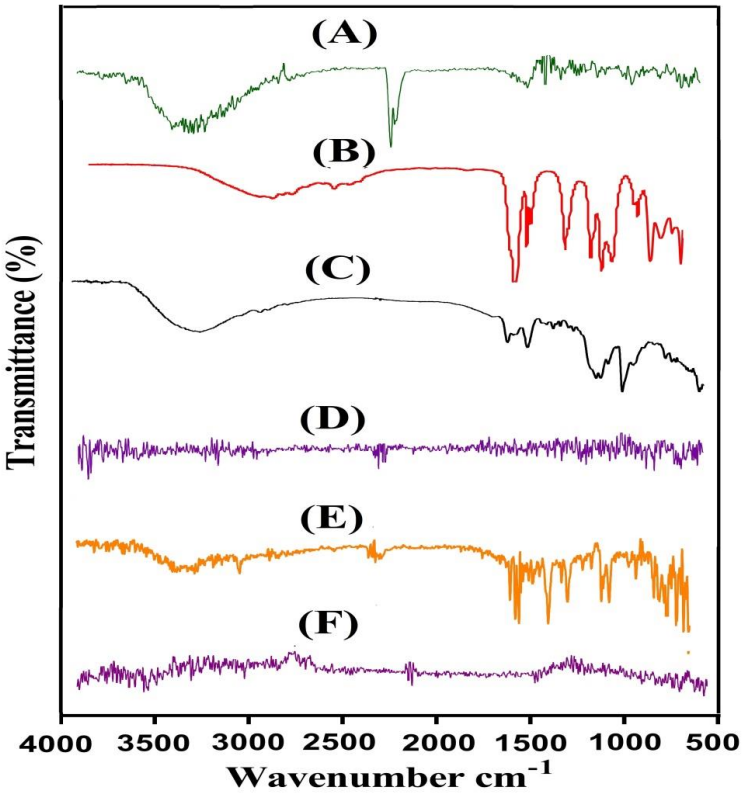

Figure 3. FTIR spectra of (**A**) PEG, (**B**) AAc, (**C**) AMPS, (**D**) unloaded PEG-co-p(AAc/AMPS) hydrogel, (**E**) KT, and (**F**) KT-loaded PEG-co-p(AAc/AMPS) hydrogel.

3.3. TGA Analysis

The thermal stability of PEG, AMPS, and PEG-co-p(AAc/AMPS) hydrogel was determined by TGA. No reduction in the weight of PEG was observed initially up to 405 °C, as perceived by the TGA of PEG (Figure 4A). A further rise in temperature resulted in a quick loss of weight of 95% at 430 °C. Higher temperatures triggered the degradation of PEG. Similarly, AMPS showed a decrease of 20% in weight at 205 °C, and a further 25% weight loss occurred at 270 °C (Figure 4B). Likewise, the decomposition of sulfonic acid was initiated at 270 °C, which persisted until the entire degradation of AMPS [37]. Similarly, weight loss of 37% was detected at 300 °C for the PEG-co-p(AAc/AMPS) hydrogel (Figure 4C). A further weight decrease of 42% was observed at 480 °C due to the breakage of functional groups of PEG (COOH) and AMPS (SO_3). Temperatures up to 485 °C led to the initial degradation of the developed PEG-based hydrogel, which continued until complete pyrolysis. Categorically, it is demonstrated from the results that the prepared hydrogels are more thermally stable than their pure contents alone. Previous study de-

veloped polymeric hydrogels from Carbopol and reported that the synthesized hydrogels were more thermally stable than their unreacted contents [38].

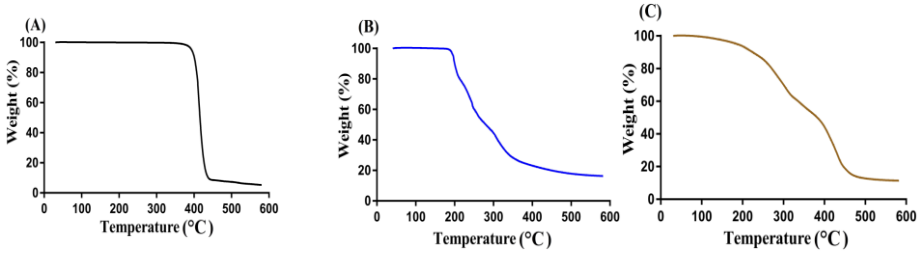

Figure 4. TGA spectra of (**A**) PEG, (**B**) AMPS, and (**C**) PEG-co-p(AAc/AMPS) hydrogel.

3.4. DSC Measurement

As shown in Figure 5A–C, the thermal stability of PEG, AMPS, and PEG-co-p(Aac/AMPS) hydrogel was evaluated by DSC. Endothermic peaks were shown at 52 and 62 °C of the unreacted PEG (Figure 5A), indicating its moisture loss. A previous study also showed the melting point of PEG at 65 °C [39]. Similarly, AMPS had an exothermic peak at 185 °C (Figure 5B), indicating dehydration, whereas a minor endothermic peak at 330 °C was detected. Higher temperatures resulted in AMPS degradation [40]. The exothermic and endothermic peaks of PEG and AMPS were altered by polymerization, as shown by the DSC of the PEG-co-p(Aac/AMPS) hydrogel (Figure 5C). Two endothermic peaks at 68 °C and 280 °C were observed. The endothermic peaks of PEG and AMPS were changed from 62 and 330 °C to 68 and 280 °C of the PEG-co-p(Aac/AMPS) hydrogel. Likewise, the exothermic peak of the monomer was shifted from 185 to 295 °C, demonstrating greater stability of the PEG-co-p(Aac/AMPS) hydrogel. Thus, the DSC spectra of fabricated hydrogel revealed increased thermal stability of PEG and AMPS after polymerization. Ganguly et al. (2011) developed PEG/chitosan-based microspheres and reported greater thermal stability for the formulated hydrogel [41], which supports our findings.

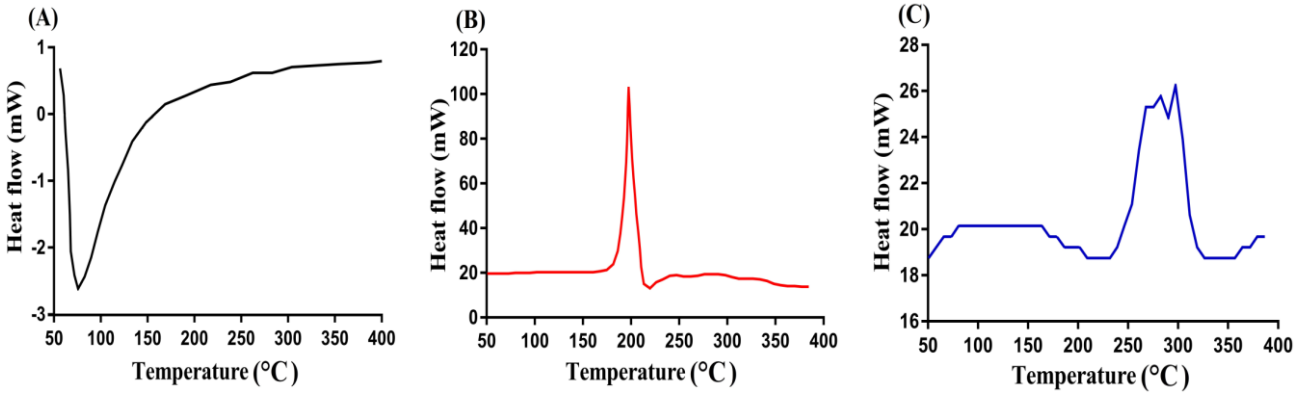

Figure 5. DSC spectra of (**A**) PEG, (**B**) AMPS, and (**C**) PEG-co-p(AAc/AMPS) hydrogel.

3.5. XRD

As shown in Figure 6, the crystallinity of the PEG and PEG-co-p(Aac/AMPS) hydrogel was perceived by XRD. Two major diffraction peaks were detected by XRD (Figure 6A) for PEG at 2θ = 14.4°, 20.1°, 22.5°, and 28.6°, demonstrating its crystalline nature. Moneghini and coworkers (2001) conducted XRD analysis of unreacted PEG-4000 and reported the crystalline nature of PEG [42]. The peaks of PEG in the current study were found to be very close to the reported peaks of PEG. A reduction in the crystallinity of PEG was observed after crosslinking with other contents of the hydrogel, as depicted by the PXRD of PEG-co-p(Aac/AMPS) hydrogel (Figure 6B). Due to the crosslinking of the hydrogel excipients, the position of peaks was changed, and certain peaks even disappeared. Corrigan et al.

(2002) prepared PEG-4000 micro-spherical particles and observed a reduction in their crystallinity [43].

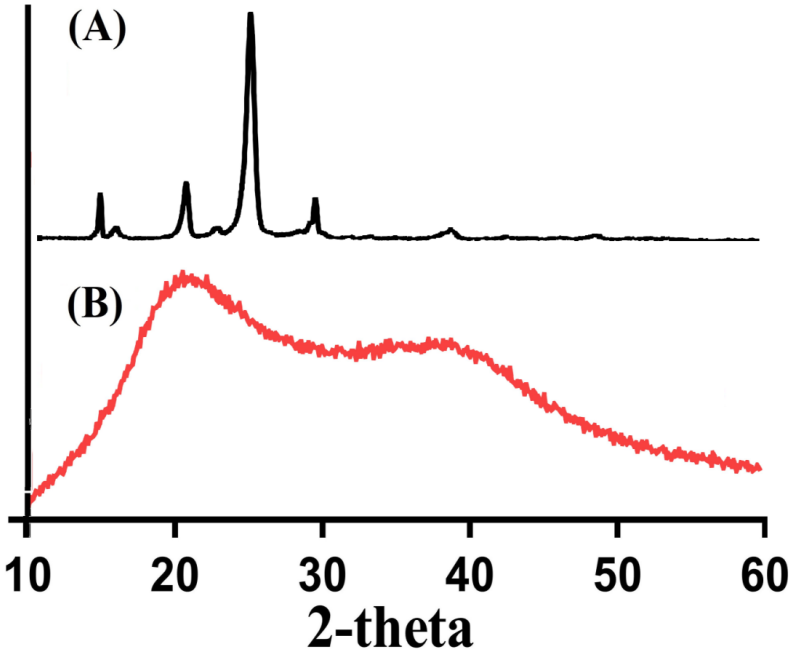

Figure 6. XRD spectra of (**A**) PEG and (**B**) PEG-co-p(Aac/AMPS) hydrogel.

3.6. SEM

The surface of the PEG-co-p(Aac/AMPS) hydrogel was uneven and had a few pores (Figure 7). The water penetrated the hydrogel, and thus, swelling of the hydrogel occurred. Strong crosslinking of hydrogel contents may result in the formation of a hard surface, which indicates the development of a compactible network of the hydrogel.

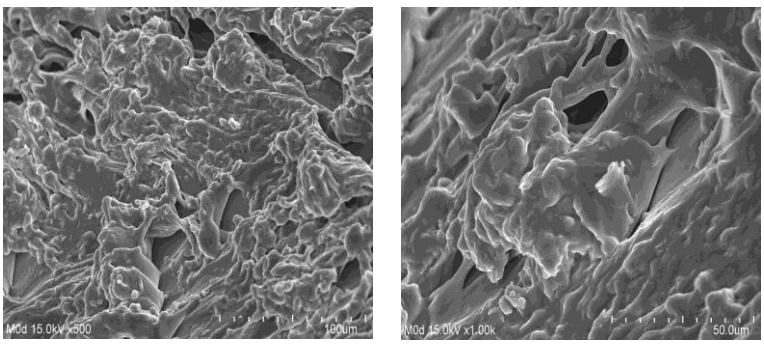

Figure 7. Scanning electron microscopy of PEG-co-p(AAc/AMPS) hydrogel.

3.7. Sol–Gel Fraction Analysis

This study was carried out to calculate the crosslinked and uncrosslinked parts of the PEG-co-p(Aac/AMPS) hydrogel. Sol is uncrosslinked and soluble, while gel is the crosslinked and insoluble part of the PEG-co-p(Aac/AMPS) hydrogel. The fractions of sol and gel were influenced by the different combinations of hydrogel components such as PEG, Aac, AMPS, and EGDMA, as shown in Figure 8A–D. The gel fraction enhanced with the increasing amount of PEG (Figure 8A). The polymerization reaction results in the generation of free radicals, which increases with greater incorporation of the polymer. Hence, the high incorporation of PEG led to the generation of more free radicals, and thus, rapid polymerization occurred and a high gel fraction was accomplished. Likewise, high concentrations of monomer contents, i.e., Aac and AMPS (Figure 8B,C), led to an enhance-

ment in the gel fraction due to the availability of many free radicals of polymer monomers. Similarly, high concentrations of EGDMA (Figure 8D) resulted in a high gel fraction. A hard compatible hydrogel network was formed with high crosslinked density, which made the prepared hydrogel more stable. Butt and coworkers prepared betacyclodextrin-based hydrogel and reported a high gel fraction with the increased incorporation of formulation excipients [44]. Likewise, Khanum and coworkers (2018) prepared HPMC hydrogel and reported a high gel fraction with the increasing composition of the polymer, crosslinker, and monomer [45]. On the other hand, the high concentrations of PEG, Aac, AMPS, and EGDMA lead to a decrease in the sol fraction due to an inverse relationship with the gel fraction [46].

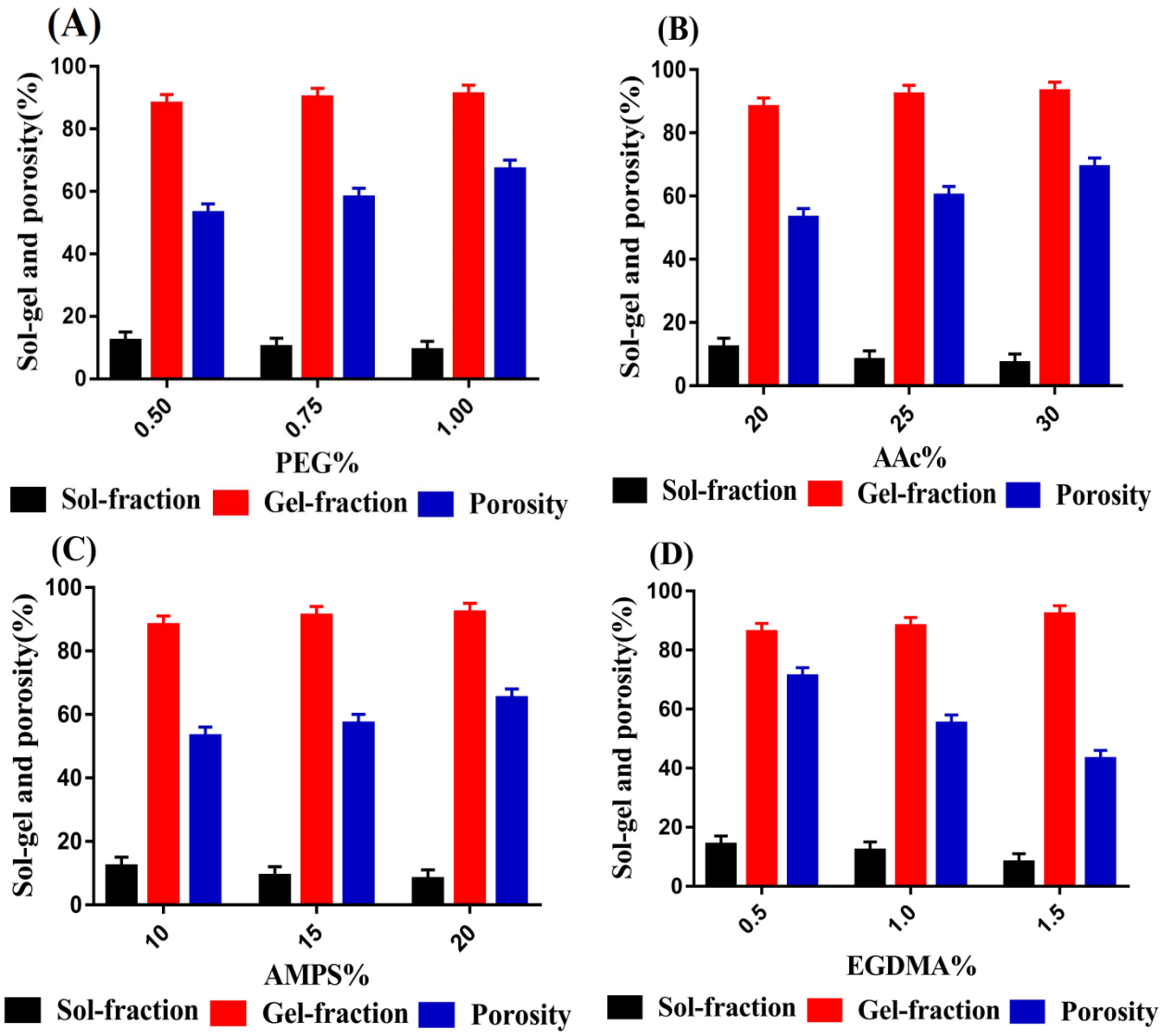

Figure 8. Effect of (**A**) PEG, (**B**) AAc, (**C**) AMPS, and (**D**) EGDMA on sol–gel fraction and porosity of PEG-co-p(Aac/AMPS) hydrogel.

3.8. Porosity

Porosity plays a crucial role in the swelling of a hydrogel and drug loading. The higher the porosity of the PEG-co-p(Aac/AMPS) hydrogel, the greater the swelling and drug loading. As shown in Figure 8A–C, high porosity was achieved with increasing incorporation of PEG, Aac, and AMPS. In the polymerization process, the viscosity of the solution increases, limiting the evaporation of gas bubbles and thus creating interconnected channels. These channels allow high water penetration into the polymeric network of the

hydrogel, and thus, high porosity was achieved with the increased incorporation of PEG, Aac, and AMPS. Contrary to PEG, Aac, and AMPS, a reduction in porosity was detected with the increased incorporation of EGDMA (Figure 8D). The reason can be correlated with the rigid and higher crosslinked network, which impedes the motility of the developed PEG-co-p(Aac/AMPS) hydrogel. Pore size was reduced, and thus, less penetration of water into the hydrogel was detected [47,48]. Thus, from this discussion, we can conclude that porosity is enhanced with higher concentrations of PEG, Aac, and AMPS, whereas it is reduced with greater incorporation of EGDMA content.

3.9. Dynamic Swelling and KT Release Evaluation

Dynamic swelling and KT release of drug-loaded PEG-co-p(Aac/AMPS) hydrogels were conducted at three pH values of 1.2, 4.6, and 7.4 to determine the pH sensitivity of the hydrogels. As shown in Figure 9A,B, greater swelling and KT release were seen at pH 4.6 and especially pH 7.4 compared to pH 1.2. A possible reason may be the deprotonation of functional groups of the polymer and monomers at high pH values. PEG contains hydroxyl (–OH) groups, which make this polymer more hydrophilic to attract a high number of water molecules. Due to the deprotonation of the –OH groups, charge density is increased, and hence a strong electrostatic repulsion occurs. Thus, expansion of the hydrogel volume was observed, and as a result, high drug release was achieved. Similarly, functional groups of Aac and AMPS were deprotonated at high pH values. Aac contains COOH groups while AMPS is composed of SO_3H groups. The deprotonation of the COOH and SO3H groups of Aac and AMPS increases the charge density, thereby enabling greater swelling and drug release due to strong electrostatic repulsion, and vice versa. On the other hand, functional groups of the polymer and monomers were protonated at pH 1.2; as a result, low swelling and KT release were observed. PEG, Aac, and AMPS functional groups conjugate with counterions through strong hydrogen bonding, resulting in detectable low swelling and KT release at pH 1.2 [37,49–52]. Like the developed hydrogel, dissolution studies were also performed for the commercial product Keten (Figure 9C). At pH 7.4, 90% of KT was released from Keten within the first 3 h, while at pH 4.6, more than 90% of KT release was perceivable within the first 5 h. Likewise, more than 96% of KT re-release was detected within 48 h at pH 1.2. Comparing the KT release from drug-loaded hydrogel and Keten, it can be easily demonstrated that KT release was prolonged for a long time by the developed hydrogel in a controlled fashion. Therefore, the designed hydrogel can be used as a promising carrier to the conventional dosage form.

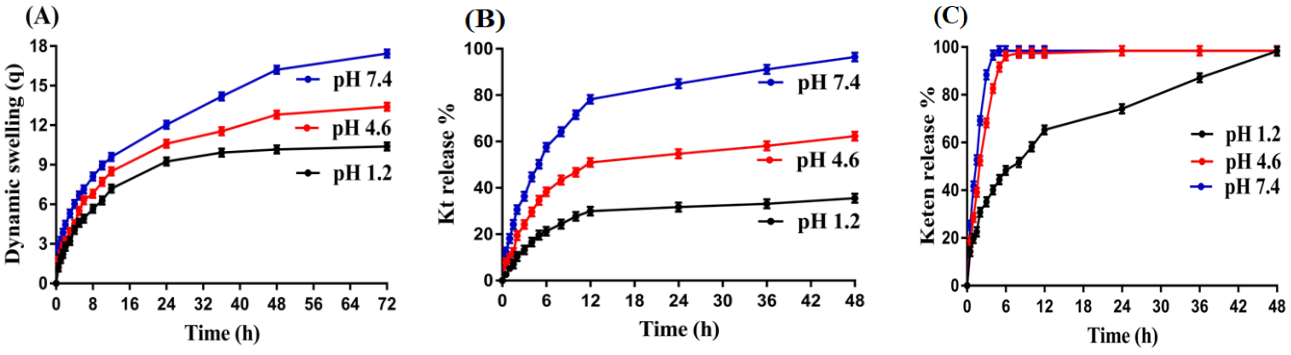

Figure 9. Effect of pH value of medium on (**A**) dynamic swelling, (**B**) drug release from PEG-co-p(AAc/AMPS) hydrogel, and (**C**) drug release from Keten.

Various kinetic models, i.e., zero-order, first-order, Higuchi, and Korsmeyer–Peppas, were applied for the determination of the release mechanism of the drug from the fabricated hydrogels. First-order "r^{2}" values were found within the range of 0.9840 and 9975, demonstrating the best-fitted data of the drug released from the developed hydrogels (Table 2) [53]. The mechanism of drug release was based on controlled diffusion. Korsmeyer et al. (1986) reported that "n" is the diffusion exponent in the Korsmeyer–Peppas model that elaborates

the mechanism of drug release [53]. Singh et al. (2007) demonstrated that the value $0.45 \leq n$ is attributed to Fickian diffusion, whereas the value $0.45 \leq n \leq 0.89$ signifies non-Fickian diffusion. Contrarily, a 0.89 value of the "n" exponent indicates typical zero-order (case II transport) release, and $n \geq 0.89$ shows super case II transport [54,55]. r and n values of all formulations were found within the ranges of 0.8273–0.9975 and 0.5047–0.6442, indicating that all formulations followed first-order kinetics with non-Fickian diffusion [54,55].

Table 2. Kinetic modeling release of Kt from PEG-co-p(AAc/AMPS) hydrogels.

F. Code	Zero-Order r^2	First-Order r^2	Higuchi r^2	Korsmeyer–Peppas	
				r^2	n
F-1	0.8725	0.9840	0.9283	0.9505	0.5462
F-2	0.8273	0.9870	0.9622	0.9431	0.5705
F-3	0.9076	0.9954	0.9735	0.9611	0.5663
F-4	0.8725	0.9840	0.9283	0.9505	0.5462
F-5	0.9652	0.9869	0.9544	0.9673	0.6066
F-6	0.9461	0.9975	0.9872	0.9897	0.6442
F-7	0.8725	0.9840	0.9283	0.9505	0.5462
F-8	0.9539	0.9935	0.9867	0.9931	0.5047
F-9	0.9454	0.9948	0.9834	0.9671	0.6039
F-10	0.9670	0.9921	0.9743	0.9788	0.5542
F-11	0.8725	0.9840	0.9283	0.9505	0.5462
F-12	0.9243	0.9872	0.9412	0.9631	0.5212

4. Conclusions

The crosslinking of the fabricated hydrogels was successfully performed using the free radical polymerization method. The structural configuration of the developed carrier system was confirmed by FTIP. An improvement in the thermal stability of the PEG and AMPS after grafting was revealed by TGA and DSC thermograms of the developed hydrogels. The crystallinity of the PEG decreased after polymerization with other hydrogel contents, as revealed by XRD analysis. SEM showed that the developed hydrogels had uneven and minor pores on their surfaces. A greater gel fraction was observed with high concentrations of the polymer, monomers, and crosslinker, whereas the sol fraction decreased. Similarly, porosity was enhanced with high feed ratios of the monomers and polymer and reduced with high feed ratios of the crosslinker. The prepared hydrogels showed pH responsiveness with high swelling and drug release at a high pH compared to a low pH. Therefore, the synthesized hydrogel can be employed as a promising excipient for controlled drug delivery.

Author Contributions: M.S.: Data curation, Formal analysis, Project administration, Writing—original draft preparation; I.-H.C.: Data curation; I.-L.L.: Data curation; M.-J.T.: Funding acquisition, Conceptualization, and Methodology; P.-C.W.: Funding acquisition, Investigation, Supervision, Writing, Conceptualization, Methodology, Supervision, and Review and editing. All authors have read and agreed to the published version of the manuscript.

Funding: This research was funded by the National Science Council of Taiwan (MOST 110-2320-B-037-014-MY2) and Tainan Municipal An-Nan Hospital (ANHRF109-14).

Conflicts of Interest: The authors declare no conflict of interest.

References

1. Sinha, V.; Kumar, R.; Singh, G. Ketorolac tromethamine formulations: An overview. *Expert Opin. Drug Deliv.* **2009**, *6*, 961–975. [CrossRef] [PubMed]
2. Alsarra, I.A.; Bosela, A.; Ahmed, S.; Mahrous, G. Proniosomes as a drug carrier for transdermal delivery of ketorolac. *Eur. J. Pharm. Biopharm.* **2005**, *59*, 485–490. [CrossRef] [PubMed]
3. Mathew, S.T.; Devi, S.G.; Sandhya, K. Formulation and evaluation of ketorolac tromethamine-loaded albumin microspheres for potential intramuscular administration. *AAPS PharmSciTech* **2007**, *8*, E100–E108. [CrossRef]

4. Wagh, P.; Mujumdar, A.; Naik, J.B. Preparation and characterization of ketorolac tromethamine-loaded ethyl cellulose micro-/nanospheres using different techniques. *Part. Sci. Technol.* **2019**, *37*, 347–357. [CrossRef]
5. Patil, J.; Rajput, R.; Patil, P.; Mujumdar, A.; Naik, J. Generation of sustained release chitosan nanoparticles for delivery of ketorolac tromethamine: A tubular microreactor approach. *Int. J. Polym. Mater. Polym. Biomater.* **2020**, *69*, 516–524. [CrossRef]
6. Rafique, N.; Ahmad, M.; Minhas, M.U.; Badshah, S.F.; Malik, N.S.; Khan, K.U. Designing gelatin-based swellable hydrogels system for controlled delivery of salbutamol sulphate: Characterization and toxicity evaluation. *Polym. Bull.* **2021**, *79*, 4535–4561. [CrossRef]
7. Peppas, N.A. *Hydrogels in Medicine and Pharmacy*; CRC Press: Boca Raton, FL, USA, 1986.
8. Brannon-Peppas, L.; Harland, R.S. *Absorbent Polymer Technology*; Elsevier: Amsterdam, The Netherlands, 2012.
9. Ahmed, E.M. Hydrogel: Preparation, characterization, and applications: A review. *J. Adv. Res.* **2015**, *6*, 105–121. [CrossRef]
10. Das, N. Preparation methods and properties of hydrogel: A review. *Int. J. Pharm. Pharm. Sci.* **2013**, *5*, 112–117.
11. Lee, K.Y.; Mooney, D.J. Hydrogels for tissue engineering. *Chem. Rev.* **2001**, *101*, 1869–1880. [CrossRef]
12. Mart, R.J.; Osborne, R.D.; Stevens, M.M.; Ulijn, R.V. Peptide-based stimuli-responsive biomaterials. *Soft Matter* **2006**, *2*, 822–835. [CrossRef]
13. Barkat, K.; Ahmad, M.; Usman Minhas, M.; Khalid, I.; Nasir, B. Development and characterization of pH-responsive polyethylene glycol-co-poly (methacrylic acid) polymeric network system for colon target delivery of oxaliplatin: Its acute oral toxicity study. *Adv. Polym. Technol.* **2018**, *37*, 1806–1822. [CrossRef]
14. Zhang, X.; Wu, D.; Chu, C.-C. Synthesis and characterization of partially biodegradable, temperature and pH sensitive Dex–MA/PNIPAAm hydrogels. *Biomaterials* **2004**, *25*, 4719–4730. [CrossRef]
15. Gemeinhart, R.A.; Park, H.; Park, K. Pore structure of superporous hydrogels. *Polym. Adv. Technol.* **2000**, *11*, 617–625. [CrossRef]
16. El-Din, H.M.N.; El-Naggar, A.W.M. Gamma radiation synthesis and swelling properties of hydrogels based on poly (ethylene glycol)/methacrylic acid (MAc) mixtures. *J. Appl. Polym. Sci.* **2010**, *117*, 1137–1143. [CrossRef]
17. Patel, R.; Patel, M. Physicochemical characterization and dissolution study of solid dispersions of lovastatin with polyethylene glycol 4000 and polyvinylpyrrolidone K30. *Pharm. Dev. Technol.* **2007**, *12*, 21–33. [CrossRef] [PubMed]
18. Sennakesavan, G.; Mostakhdemin, M.; Dkhar, L.; Seyfoddin, A.; Fatihhi, S. Acrylic acid/acrylamide based hydrogels and its properties-A review. *Polym. Degrad. Stab.* **2020**, *180*, 109308. [CrossRef]
19. Suhail, M.; Xie, A.; Liu, J.-Y.; Hsieh, W.-C.; Lin, Y.-W.; Minhas, M.U.; Wu, P.-C. Synthesis and In Vitro Evaluation of Aspartic Acid Based Microgels for Sustained Drug Delivery. *Gels* **2021**, *8*, 12. [CrossRef] [PubMed]
20. Ullah, K.; Sohail, M.; Buabeid, M.A.; Murtaza, G.; Ullah, A.; Rashid, H.; Khan, M.A.; Khan, S.A. Pectin-based (LA-co-MAA) semi-IPNS as a potential biomaterial for colonic delivery of oxaliplatin. *Int. J. Pharm.* **2019**, *569*, 118557. [CrossRef] [PubMed]
21. Suhail, M.; Hsieh, Y.H.; Khan, A.; Minhas, M.U.; Wu, P.C. Preparation and In Vitro Evaluation of Aspartic/Alginic Acid Based Semi-Interpenetrating Network Hydrogels for Controlled Release of Ibuprofen. *Gels* **2021**, *7*, 68. [CrossRef]
22. Ullah, K.; Sohail, M.; Mannan, A.; Rashid, H.; Shah, A.; Murtaza, G.; Khan, S.A. Facile synthesis of chitosan based-(AMPS-co-AA) semi-IPNs as a potential drug carrier: Enzymatic degradation, cytotoxicity, and preliminary safety evaluation. *Curr. Drug Deliv.* **2019**, *16*, 242–253. [CrossRef]
23. Sarfraz, R.; Khan, H.; Mahmood, A.; Ahmad, M.; Maheen, S.; Sher, M. Formulation and evaluation of mouth disintegrating tablets of atenolol and atorvastatin. *Indian J. Pharm. Sci.* **2015**, *77*, 83. [CrossRef] [PubMed]
24. Ullah, K.; Khan, S.A.; Murtaza, G.; Sohail, M.; Manan, A.; Afzal, A. Gelatin-based hydrogels as potential biomaterials for colonic delivery of oxaliplatin. *Int. J. Pharm.* **2019**, *556*, 236–245. [CrossRef] [PubMed]
25. Zia, M.A.; Sohail, M.; Minhas, M.U.; Sarfraz, R.M.; Khan, S.; de Matas, M.; Hussain, Z.; Abbasi, M.; Shah, S.A.; Kousar, M. HEMA based pH-sensitive semi IPN microgels for oral delivery; a rationale approach for ketoprofen. *Drug Dev. Ind. Pharm.* **2020**, *46*, 272–282. [CrossRef] [PubMed]
26. Ijaz, H.; Tulain, U.R.; Azam, F.; Qureshi, J. Thiolation of arabinoxylan and its application in the fabrication of pH-sensitive thiolated arabinoxylan grafted acrylic acid copolymer. *Drug Dev. Ind. Pharm.* **2019**, *45*, 754–766. [CrossRef]
27. Hussain, A.; Khalid, S.; Qadir, M.; Massud, A.; Ali, M.; Khan, I.; Saleem, M.; Iqbal, M.; Asghar, S.; Gul, H. Water uptake and drug release behaviour of methyl methacrylate-co-itaconic acid [P (MMA/IA)] hydrogels cross-linked with methylene bis-acrylamide. *J. Drug Deliv. Sci. Technol.* **2011**, *21*, 249. [CrossRef]
28. Peppas, N.A.; Sahlin, J.J. A simple equation for the description of solute release. III. Coupling of diffusion and relaxation. *Int. J. Pharm.* **1989**, *57*, 169–172. [CrossRef]
29. Patil, M.P.; Gaikwad, N.J. Priprava i karakterizacija gliklazid-polietilen glikol 4000 čvrstih disperzija. *Acta Pharm.* **2009**, *59*, 57–65.
30. Moharram, M.; Khafagi, M. Application of FTIR spectroscopy for structural characterization of ternary poly (acrylic acid)–metal–poly (vinyl pyrrolidone) complexes. *J. Appl. Polym. Sci.* **2007**, *105*, 1888–1893. [CrossRef]
31. Azmeera, V.; Adhikary, P.; Krishnamoorthi, S. Synthesis and characterization of graft copolymer of dextran and 2-acrylamido-2-methylpropane sulphonic acid. *Int. J. Carbohydr. Chem.* **2012**, *2012*, 209085. [CrossRef]
32. Suhail, M.; Ullah, H.; Vu, Q.L.; Khan, A.; Tsai, M.J.; Wu, P.C. Preparation of pH-Responsive Hydrogels Based on Chondroitin Sulfate/Alginate for Oral Drug Delivery. *Pharmaceutics* **2022**, *14*, 2110. [CrossRef]
33. Begum, M.Y.; Shaik, M.R.; Abbulu, K.; Sudhakar, M.; Reddy, M. Ketorolac tromethamine loaded liposomes of long alkyl chain lipids: Development, characterization and in vitro performance. *Int. J. Pharm. Tech. Res.* **2012**, *4*, 218–255.

34. Waghulde, M.; Mujumdar, A.; Naik, J. Preparation and characterization of miglitol-loaded Poly (d, l-lactide-co-glycolide) microparticles using high pressure homogenization-solvent evaporation method. *Int. J. Polym. Mater. Polym. Biomater.* **2019**, *68*, 198–207. [CrossRef]
35. Aşık, M.D.; Uğurlu, N.; Yülek, F.; Tuncer, S.; Türk, M.; Denkbaş, E.B. Ketorolac tromethamine loaded chitosan nanoparticles as a nanotherapeutic system for ocular diseases. *Hacet. J. Biol. Chem.* **2013**, *41*, 81–86.
36. Patil, J.S.; Yadava, S.; Mokale, V.J.; Naik, J.B. Preparation and characterization of single pulse sustained release ketorolac nanoparticles to reduce their side-effects at gastrointestinal tract. In Proceedings of the International Conference on Advances in Chemical Engineering, Kollam, India, 16–18 October 2014; pp. 59–62.
37. Khalid, I.; Ahmad, M.; Minhas, M.U.; Barkat, K. Synthesis and evaluation of chondroitin sulfate based hydrogels of loxoprofen with adjustable properties as controlled release carriers. *Carbohydr. Polym.* **2018**, *181*, 1169–1179. [CrossRef] [PubMed]
38. Singh, B.; Dhiman, A. Functionalization of carbopol with NVP for designing antibiotic drug loaded hydrogel dressings for better wound management. *J. Pharm. Biopharm. Res.* **2019**, *1*, 1–14. [CrossRef]
39. Guleria, R.; Kaith, N.; Singh, R. Peg based solid dispersions of gliclazide: A comparative study. *Int. J. Pharm. Pharm. Sci.* **2012**, *4*, 507–511.
40. Qiao, J.L.; Hamaya, T.; Okada, T. New highly proton-conducting membrane poly(vinylpyrrolidone)(PVP) modified poly(vinyl alcohol)/2-acrylamido-2-methyl-1-propanesulfonic acid (PVA-PAMPS) for low temperature direct methanol fuel cells (DMFCs). *Polymer* **2005**, *46*, 10809–10816. [CrossRef]
41. Ganguly, K.; Aminabhavi, T.M.; Kulkarni, A.R. Colon targeting of 5-fluorouracil using polyethylene glycol cross-linked chitosan microspheres enteric coated with cellulose acetate phthalate. *Ind. Eng. Chem. Res.* **2011**, *50*, 11797–11807. [CrossRef]
42. Moneghini, M.; Kikic, I.; Voinovich, D.; Perissutti, B.; Filipović-Grčić, J. Processing of carbamazepine–PEG 4000 solid dispersions with supercritical carbon dioxide: Preparation, characterisation, and in vitro dissolution. *Int. J. Pharm.* **2001**, *222*, 129–138. [CrossRef]
43. Corrigan, D.O.; Healy, A.M.; Corrigan, O.I. The effect of spray drying solutions of polyethylene glycol (PEG) and lactose/PEG on their physicochemical properties. *Int. J. Pharm.* **2002**, *235*, 193–205. [CrossRef]
44. Butt, H.; Minhas, M.U.; Khan, K.U.; Sohail, M.; Khalid, I.; Rehmani, S.; Suhail, M. Cross-linking polymerization of beta-cyclodextrin with acrylic monomers; characterization and study of drug carrier properties. *Polym. Bull.* **2022**, *80*, 1893–1914. [CrossRef]
45. Khanum, H.; Ullah, K.; Murtaza, G.; Khan, S.A. Fabrication and in vitro characterization of HPMC-g-poly (AMPS) hydrogels loaded with loxoprofen sodium. *Int. J. Biol. Macromol.* **2018**, *120*, 1624–1631. [CrossRef] [PubMed]
46. Dergunov, S.A.; Nam, I.K.; Mun, G.A.; Nurkeeva, Z.S.; Shaikhutdinov, E.M. Radiation synthesis and characterization of stimuli-sensitive chitosan–polyvinyl pyrrolidone hydrogels. *Radiat. Phys. Chem.* **2005**, *72*, 619–623. [CrossRef]
47. Yin, L.; Fei, L.; Cui, F.; Tang, C.; Yin, C. Superporous hydrogels containing poly (acrylic acid-co-acrylamide)/O-carboxymethyl chitosan interpenetrating polymer networks. *Biomaterials* **2007**, *28*, 1258–1266. [CrossRef]
48. Ranjha, N.M.; Qureshi, U.F. Preparation and characterization of crosslinked acrylic acid/hydroxypropyl methyl cellulose hydrogels for drug delivery. *Int. J. Pharm. Pharm. Sci.* **2014**, *6*, 410.
49. Sohail, M.; Ahmad, M.; Minhas, M.U.; Ali, L.; Munir, A.; Khalid, I. Synthesis and characterization of graft PVA composites for controlled delivery of valsartan. *Lat. Am. J. Pharm.* **2014**, *33*, 1237–1244.
50. Chen, S.-C.; Wu, Y.-C.; Mi, F.-L.; Lin, Y.-H.; Yu, L.-C.; Sung, H.-W. A novel pH-sensitive hydrogel composed of N, O-carboxymethyl chitosan and alginate cross-linked by genipin for protein drug delivery. *J. Control. Release* **2004**, *96*, 285–300. [CrossRef]
51. Malik, N.S.; Ahmad, M.; Minhas, M.U.; Tulain, R.; Barkat, K.; Khalid, I.; Khalid, Q. Chitosan/Xanthan Gum Based Hydrogels as Potential Carrier for an Antiviral Drug: Fabrication, Characterization, and Safety Evaluation. *Front. Chem.* **2020**, *8*, 50. [CrossRef]
52. Lim, S.L.; Tang, W.N.H.; Ooi, C.W.; Chan, E.S.; Tey, B.T. Rapid swelling and deswelling of semi-interpenetrating network poly(acrylic acid)/poly(aspartic acid) hydrogels prepared by freezing polymerization. *J. Appl. Polym. Sci.* **2016**, *133*, 43515. [CrossRef]
53. Korsmeyer, R.W.; Von Meerwall, E.; Peppas, N.A. Solute and penetrant diffusion in swellable polymers. II. Verification of theoretical models. *J. Polym. Sci. Part B Polym. Phys.* **1986**, *24*, 409–434. [CrossRef]
54. Shoaib, M.H.; Tazeen, J.; Merchant, H.A.; Yousuf, R.I. Evaluation of drug release kinetics from ibuprofen matrix tablets using HPMC. *Pak. J. Pharm. Sci.* **2006**, *19*, 119–124. [PubMed]
55. Maziad, N.A.; El-Hamouly, S.; Zied, E.; El Kelani, T.A.; Nasef, N.R. Radiation preparation of smart hydrogel has antimicrobial properties for controlled release of ciprofloxacin in drug delivery systems. *Asian J. Pharm. Clin. Res.* **2015**, *14*, 15.